Acetone Absorption in Irradiated Polycarbonate

Terhou Wu,[†] Sanboh Lee,*[,†] and Wen-Chang Chen[‡]

Department of Materials Science, National Tsing Hua University, and Polymer Science and Technology Division, Union Chemical Laboratories, Industrial Technology Research Institute, Hsinchu, Taiwan, Republic of China

Received February 22, 1995; Revised Manuscript Received June 5, 1995[⊗]

ABSTRACT: Acetone absorption in irradiated polycarbonate was investigated. The molecular weight and glass transition temperature of polycarbonate decreased with increasing the γ-ray dose. Experimental data obtained from acetone transport in polycarbonate with various doses correlated sufficiently well with Harmon's model which was accounted for case I, case II, and anomalous transport. The diffusion coefficient for case I, velocity for case II, and diffusion coefficient for diffusion front satisfied the Arrhenius plot for all γ-ray doses. The equilibrium solubility satisfied the van't Hoff plot regardless of the γ-ray dose. Additionally, in the low-temperature range activation energies of case I, case II and the diffusion front, and the heat of mixing were found to have the same value for doses greater than 100 kGy which was different from those for unirradiated polycarbonate. This observation implied that acetone transport in irradiated polycarbonate occurs via the same mechanism for doses greater than 1000 kGy. The equilibrium solubility and diffusion coefficient for diffusion front at a given temperature were the same for all doses in the high-temperature range.

1. Introduction

Two groups of linear polymers are categorized on the basis of their exposure to high-energy irradiation.[1] The formation of intermolecular cross-links leads to a radiation-induced increase in molecular weight in group I. Polyethylene, polypropylene, poly(methyl acrylate), polystyrene, etc., belong to group I. Irradiated polymers of group II degrade (or undergo scission) so that molecular weights decrease with radiation dose. Polyisobutylene, poly(methyl methacrylate), poly(vinylidene chloride), polycarbonate, etc., belong to group II. In comparison with many other polymers, polycarbonates are highly resistant to radiation. Low doses of γ-irradiation (below 50 kGy) increase the molecular weight of polycarbonate and enhance its physical properties[2] because γ-rays do not have enough energy to scissor the polymer chain and monomers gain energy from γ-rays to react with polymer chains. Harrington and Giberson[3] and Giberson[4] reported similar behavior for polycarbonate irradiated with γ-rays from a cobalt-60 source in air and under vacuum pressure. Barker et al.[5] studied many physical and chemical properties of irradiated Lexan polycarbonate, e.g., color center destruction by oxygen diffusion, optical absorption spectrum, dielectric characteristics, and EPR spectrum. However, the mass transport in irradiated polycarbonate has not yet been addressed.

The transport of organic solvents in amorphous glassy polymers has been the subject of much attention. Both case I (concentration-gradient-controlled) and case II (stress-relaxatin-controlled) contribute to the rate and extent of penetrant sorption in polymers.[6–8] An extensive range of behavior patterns may be encountered as the relative contribution of these two processes changes. These observed phenomena vary not only from system to system but also with the temperature and concentration intervals in a given penetrant–polymer pair.[9] Case II transport is often accompanied with the sharp front which is linearly proportional to time.[10–12] Hopfenberg and Frisch[13] suggested that behavior ranging from case I to limiting case II sorption is expected for any given penetrant–polymer system if a sufficient range of temperature and penetrant activity is traversed experimentally. Ware et al.[14] investigated the diffusion of three solvents in polycarbonate, finding that only metha-

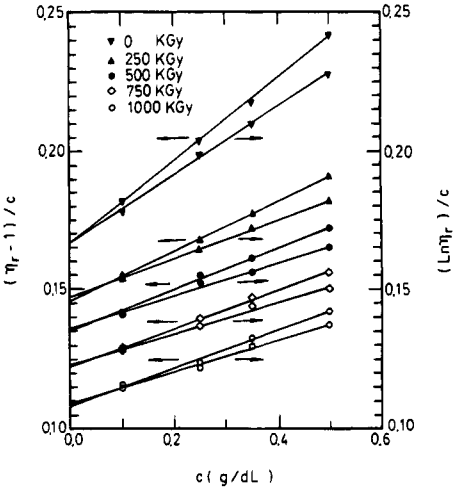

Figure 1. Plots of reduced specific viscosity versus concentration for various doses.

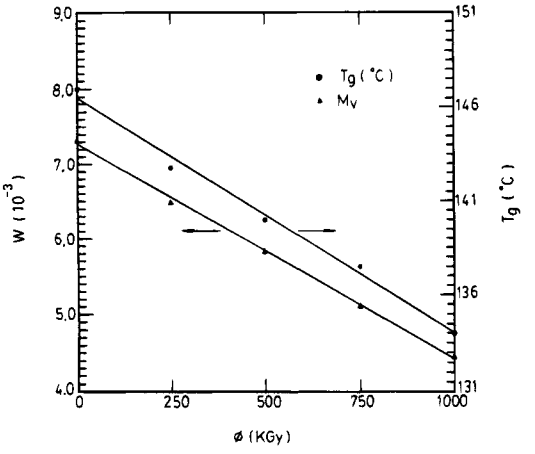

Figure 2. Molecular weight and glass transition temperature as a function of γ-ray dose.

* To whom correspondence should be addressed.
† National Tsing Hua University.
‡ Industrial Technology Research Institute.
⊗ Abstract published in *Advance ACS Abstracts,* July 15, 1995.

0024-9297/95/2228-5751$09.00/0

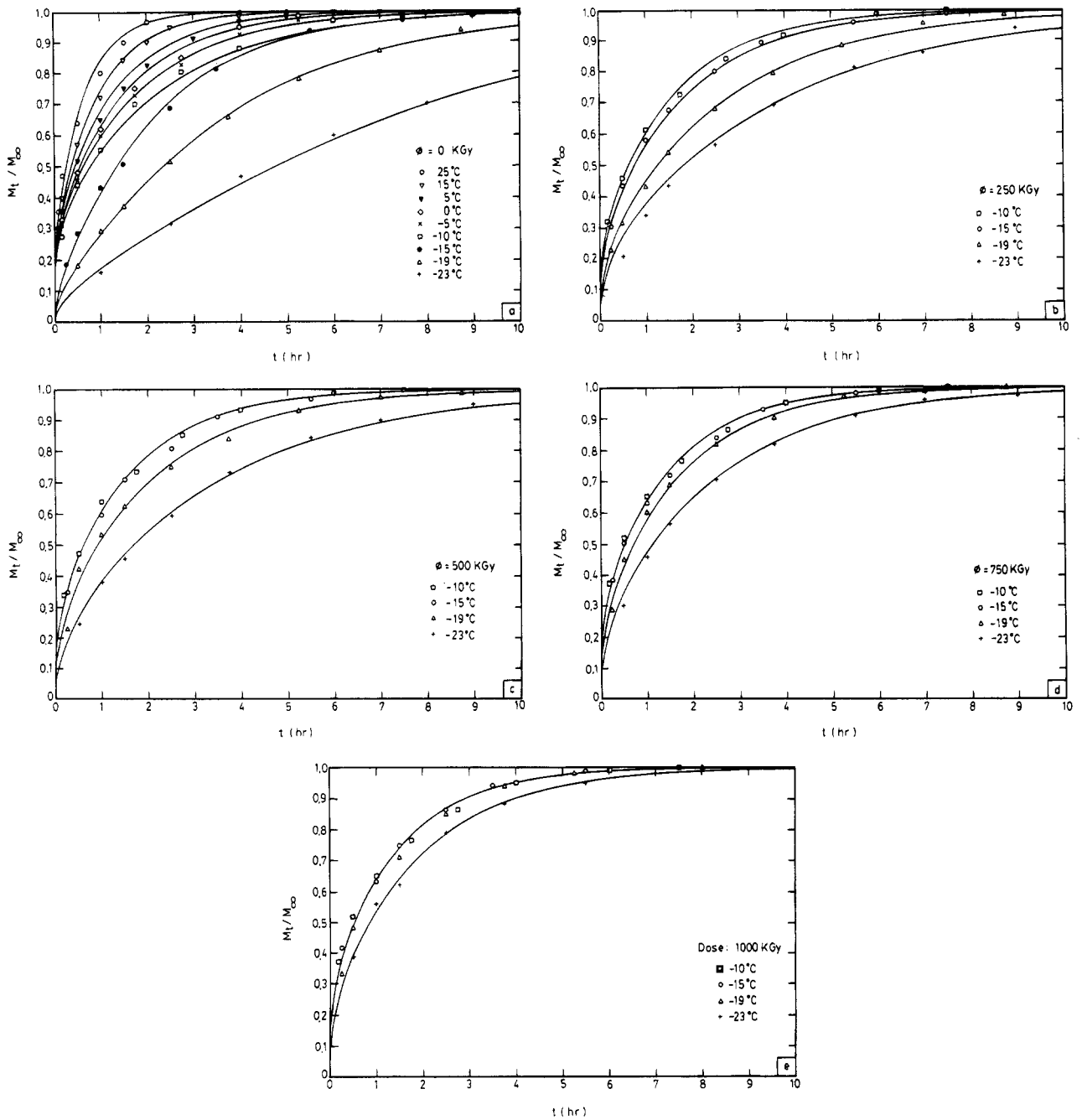

Figure 3. Acetone absorption in irradiated polycarbonate: (a) $\phi = 0$, (b) 250, (c) 500, (d) 750, and (e) 1000 kGy.

nol exhibited pure case I transport. Miller et al.[15] reported square root of time dependency in mass uptake of carbon tetrachloride in polycarbonate at 25 °C; however, they ignored the initial sorption period. The diffusion front of several penetrants in polycarbonate was observed to proceed with as $t^{1/2}$ where t is time.[16-18]

Kwei and co-workers[19-23] proposed a model for mass transport in polymeric materials which accounted for case I (concentration-gradient-controlled), case II (stress-relaxation-controlled), and anomalous absorption (mixed case I with case II). Their equation was modified by Harmon et al.,[24,25] who studied methanol transport in deformed poly(methyl methacrylate) (PMMA). The direction of case II is the same as that of case I in PMMA. When the penetrant sorbs in the PMMA, PMMA does not change its microstructure. However, solvent transport in polycarbonate is significantly different from that in PMMA. Solvent sorption in polycarbonate results in a change from the amorphous state to the crystalline state.[15,17,26-30] Recently, carbon tetrachloride-induced crack healing in polycarbonate was studied in which carbon tetrachloride was absorbed by case I transport but squeezed out by case II transport I.[31] This has prompted an investigation here of the acetone absorption in irradiated polycarbonate.

2. Experimental Procedure

Polycarbonate, Lexan 9034, was obtained from General Electric Co. in the form of a 2.03-mm-thick cast sheet. Rectangular samples of dimensions 20 × 10 × 1 mm were prepared for the absorption study and solvent front measurement. These samples were polished on 600 and 1200 grit carbimet papers and with 1 and 0.05 μm aluminum slurries. Samples were annealed in vacuum at 130 °C for 24 h and furnace cooled to room temperature in order to release residual stresses. Samples were then exposed in air at ambient temperature to γ-ray dose of 14.2 kGy/h from a 3000 Ci cobalt-60 source at Isotope Center, National Tsing Hua University.

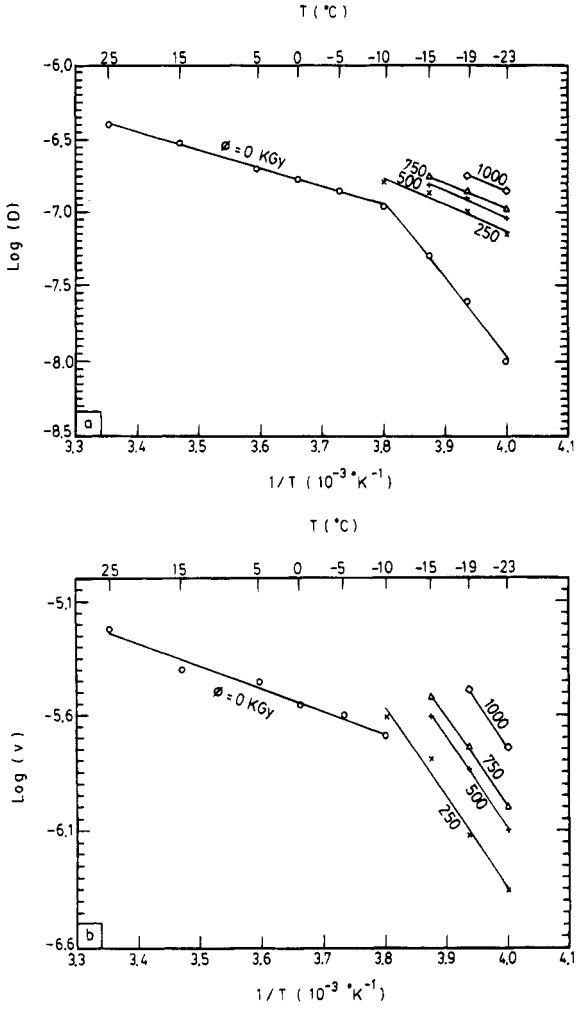

Figure 4. Arrhenius plots of (a) D and (b) positive v for different doses.

Samples were exposed to doses 250, 500, 750, and 1000 kGy, respectively.

Intrinsic viscosity samples were dissolved in methyl chloride at ambient temperature to yield solutions of concentrations between 0.1 and 0.5 g/dL. The intrinsic viscosity was measured using the Ubbelohde capillary viscometer in a refrigerated circulating bath maintained at 20 ± 0.1 °C. The efflux time was determined at least 10 times until the reading agreed within 0.1% error of their mean. Glass transition temperature samples were produced by cutting a layer of thickness approximately 0.3 mm from the cast sheet and then, after polishing, punching out disks of 5 mm diameter. The resulting disks of roughly 10 mg were exposed in air to γ-rays for different durations to reach the desired dose. Each sample was enclosed in a regular aluminum pan and placed in a Seiko 1 SSC-500 differential scanning calorimeter for measurement at a scanning rate of 5 °C/min The specimens were heated from ambient temperature to 180 °C at a heating rate of 5 °C/min.

Each absorption study sample was preweighed. Doses for the absorption study were the same as those in the intrinsic viscosity and glass transition temperature studies. The samples were preheated to the test temperature and moved to an acetone-filled glass bottle at the same temperature, maintained by means of a refrigerated circulating bath at −23 to ~25 °C. Following each experimental interval of immersion, the sample was removed. Its surfaces were blotted free of surplus acetone, and its mass was measured using a Kern 870 digital balance. After being weighed, the sample was discarded because of solvent-induced crack nucleation. The sharp front kinetics were similar to those of the absorption study. At a desired period, the sample was removed, cleaved, and

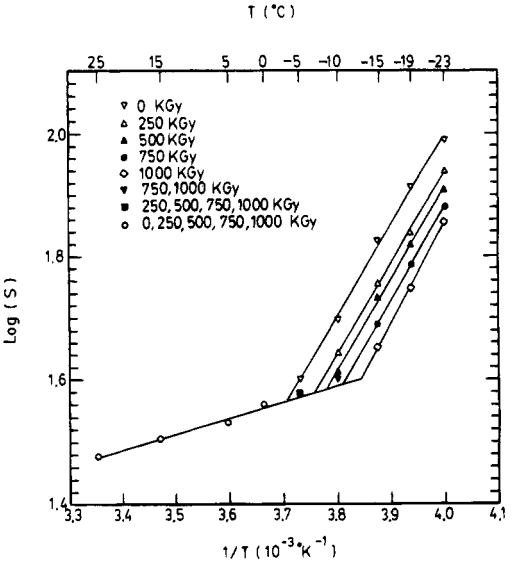

Figure 5. van't Hoff plots of acetone solubility in irradiated polycarbonate with various doses.

observed immediately using a Mitutoyo MVK-G1 hardness tester to determine the sharp front.

3. Results and Discussion

3.1. DSC and Viscosity Studies. Based on the viscosity study, Figure 1 shows the reduced specific viscosity $(\eta_r - 1)/c$ or $\mathrm{Ln}(\eta_r)/c$ of irradiated polycarbonate versus the concentration c of methylene chloride. For a given dose, the specific viscosity versus concentration plot is linear, following a least-squares fit. The intrinsic viscosity $[\eta]$ was obtained as the average of the ordinate intercepts of $(\eta_r - 1)/c$ and $\mathrm{Ln}(\eta_r)/c$ at $c = 0$.[32] The molecular weight W was calculated from the intrinsic viscosity $[\eta]$ by using the Staudinger−Kuhn correction, i.e.

$$[\eta] = KW^a \tag{1}$$

where K and a are constants.[33] The plot of molecular weight W versus dose ϕ for irradiated polycarbonate is shown in Figure 2 where K and a are 0.92×10^{-5} and 0.87, respectively, as obtained from Schulz and Horbach.[34] The plot is over a broad range of doses. The glass transition temperature T_g is shown in Figure 2 as a function of dose ϕ. This figure indicates that the glass transition temperature decreases with increasing dose. The glass transition temperature increases with molecular weight over the molecular weight range encountered here.[35] Both the measurements of intrinsic viscosity and glass transition temperature confirm that radiation induces degradation or scission of polycarbonate chains and decreases the molecular weight. The irradiation appears to have caused a significant amount of scission reactions which lowers the molecular weight of polycarbonatee or the production of monomers which plasticize the matrix, lowering the T_g and the viscosity of the system. It is different from the fact that low doses (below 50 kGy) increase with the molecular weight of polycarbonate[2] because a γ-ray does not afford enough energy to scissor the polymer chain and monomers gain energy from a γ-ray to react with the polymer chain.

3.2. Acetone Transport. The data for acetone transport in irradiated polycarbonate at temperatures ranging from −23 to +25 °C are shown in parts a−e of Figure 3. These data can be curve-fitted by a model proposed by Harmon et al.[24] Acetone transport in

polycarbonate is assumed to be accounted for by case I, case II, and anomalous sorption. The characteristic parameters corresponding to cases I and II are D for diffusion coefficient and v for velocity, respectively. The polycarbonate is initially assumed to be free of acetone, and the concentration of acetone is maintained constant on the surface boundaries at all times. The weight of acetone M_t based on the one-dimensional Harmon's model[24] is

$$\frac{M_t}{M_\infty} = 1 - 2\sum_{n=1}^{\infty} \frac{\lambda_n^2[1 - 2\cos\lambda_n e^{-vl/2D}]}{\beta_n^4\left[1 - \frac{2D}{vl}\cos^2\lambda_n\right]} e^{-\beta_n^2 Dt/l^2} \quad (2)$$

where

$$\lambda_n = \frac{vl}{2D}\tan\lambda_n \quad (3)$$

$$\beta_n^2 = \frac{v^2l^2}{4D^2} + \lambda_n^2 \quad (4)$$

$2l$ is the total thickness of the specimen and M_∞ is the equilibrium weight of acetone, obtained at the time reaching infinity. The solid lines in Figure 3 are plotted using eq 2. This figure reveals that the theoretical curve correlates sufficiently well with the experimental data. For doses 500 and 750 kGy the data at −10 °C cannot be distinguished from those at −15 °C. Distinguishing between the data for doses 1000 kGy at temperatures above −19 °C is relatively difficult. Both D and v at different temperatures with various doses are plotted in parts a and b of Figure 4, respectively. These figures indicate that they satisfy the Arrhenius equation. The activation energies for D in unirradiated polycarbonate ($\phi = 0$) are 12 and 50 kcal/mol corresponding to temperatures $T \geq -10$ °C and $T < -10$ °C, respectively; in addition, the activation energies for D in irradiated polycarbonate are 18, 18, 17, and 17 kcal/mol corresponding to $\phi = 250$, 500, 750, and 1000 kGy, respectively. The activation energies for D of irradiated polycarbonate are smaller than that of unirradiated polycarbonate in the same temperature range. Equation 2 and Figure 4b confirm that v is positive. The sign of v indicates the direction of case II. The positive sign implies the flux of case II moves from the center to the outer surface; in addition, the negative sign has the opposite trend to the positive sign. This is in contrast with the observed phenomenon of poly(methyl methacrylate) (PMMA) in which both case I and case II transports move from the outer surface to the center,[24,25,36] v is negative. This difference arises from the microstructural change in the acetone−polycarbonate system; however, no change occurs in the penetrant−PMMA system. According to Figure 4b the activation energies for v in unirradiated polycarbonate ($\phi = 0$) are 10 kcal/mol in the temperature range $T > -10$ °C. Furthermore, the activation energies for v in irradiated polycarbonate are 37, 38, 37, and 39 kcal/mol corresponding to $\phi = 250$, 500, 750, and 1000 kGy, respectively. The activation energies of v with various doses are quite similar. Note that, at the temperatures $T < -15$ °C, the value of v in unirradited polycarbonate is the same as that of irradiated polycarbonate $\phi = 750$ kGy with the exception of the signs.

3.3. Solubility. The equilibrium solubilities (S) of acetone in polycarbonate at different temperatures for various doses are plotted in Figure 5 and satisfy the van't Hoff equation. The acetone transport in polycarbonate is an exothermic process, as indicated from the positive slope in Figure 5. This is due to the structural change. Three remarkable features are worth mentioning. First, at high temperatures, the solubility is almost the same for all doses; in addition, at low temperatures the difference in solubility with dose is pronounced. The transition temperatures T_s's of slope change in Figure 5, as determined by the intercept of two lines with different slopes, are −3, −7, −9, −11, and −13 °C for $\phi = 0$, 250, 500, 750, and 1000 kGy, respectively. T_s decreases with increasing dose. Second, in the low-temperature range (-23 °C $\leq T < T_s$), the equilibrium solubility decreases with increasing dose at the same temperature, while the slope remains almost un-

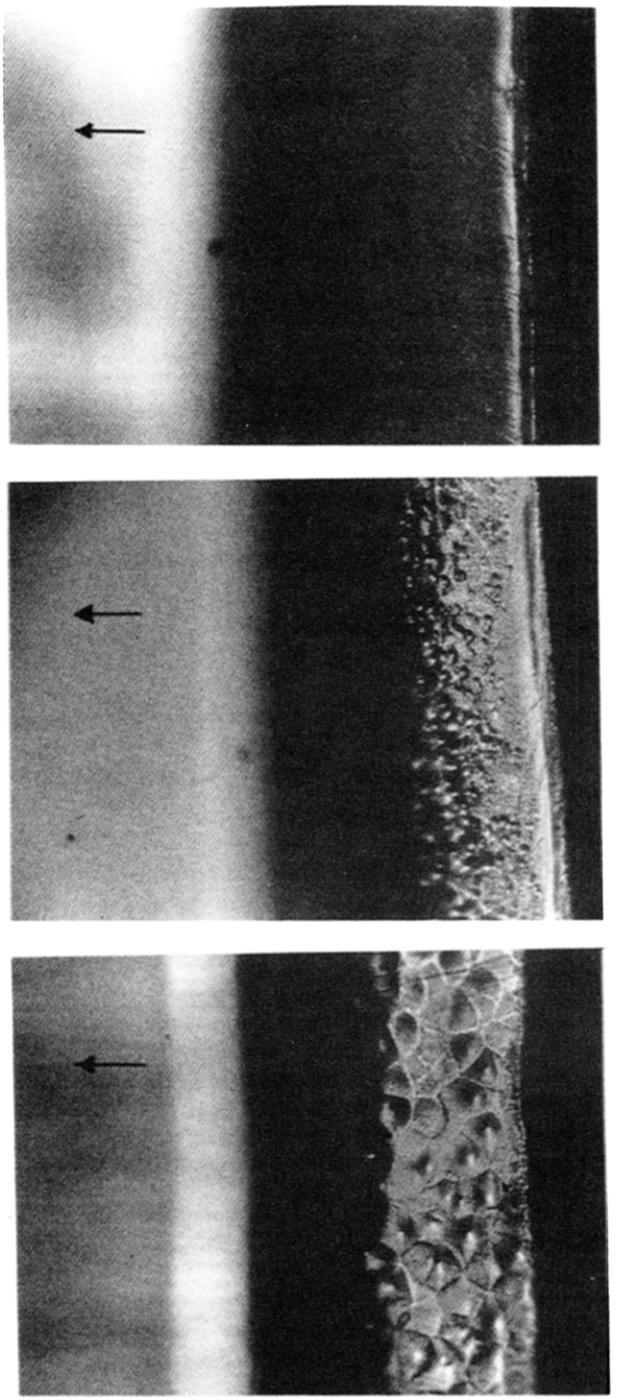

Figure 6. Microscopic image of polycarbonate saturated with acetone at (a) −19 (200×), (b) −10 (200×), and (c) 25 °C (200×).

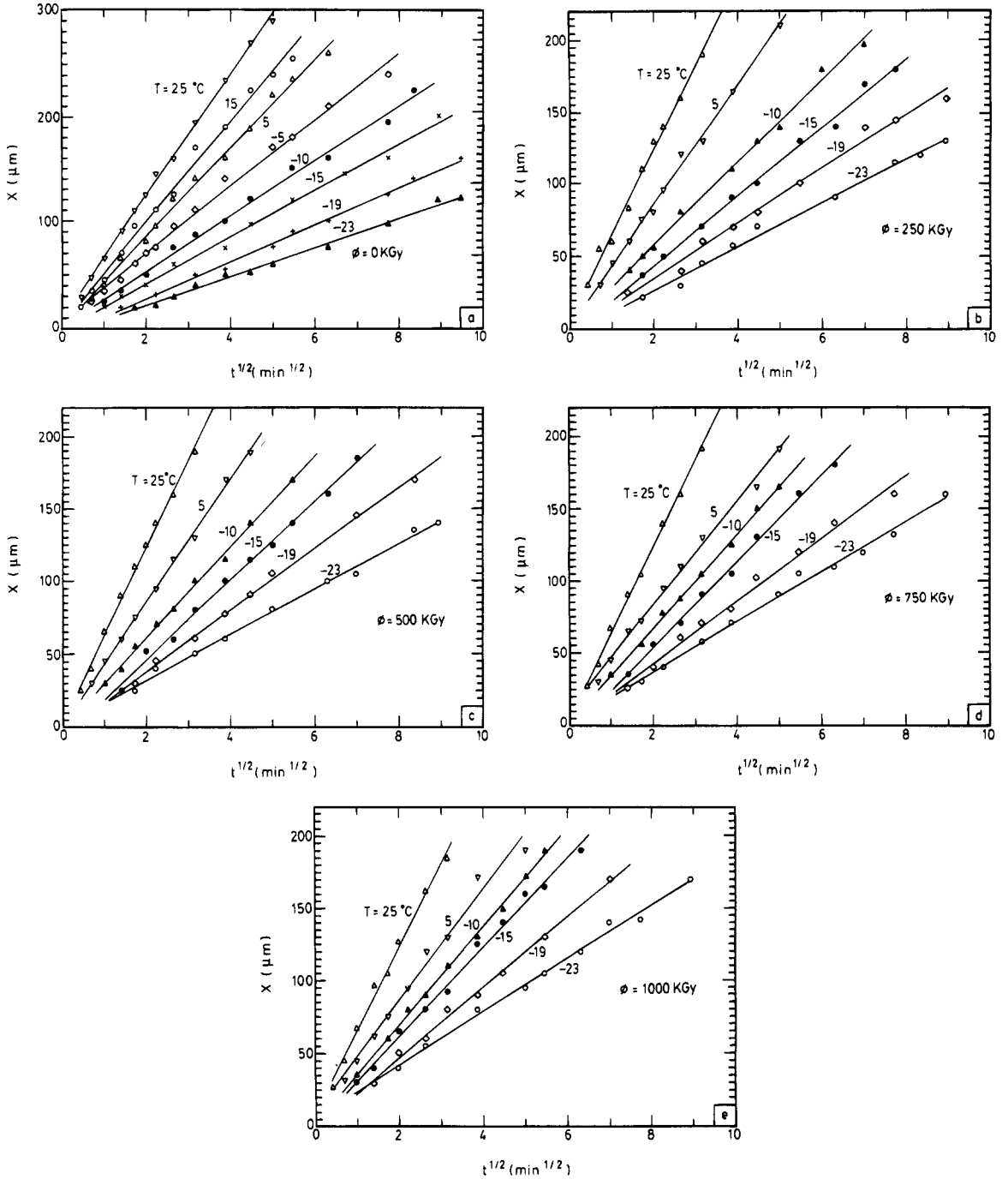

Figure 7. Distance from the diffusion front to the free surface as a function of time for various doses: (a) $\phi = 0$, (b) 250, (c) 500, (d) 750, and (e) 1000 kGy, respectively.

changed. This is attributed to solvent-induced crystallization. The polycarbonate crystallizes more easily and has more spherulites at lower molecular weights than at higher molecular weights. The heats of mixing are −6.8, −6.8, −6.8, −6.9, and −7.3 kcal/mol for $\phi = 0$, 250, 500, 750, and 1000 kGy, respectively. The negative heat of mixing is also accounted for by the formation of spherulites since crystallization is an exothermic process. Acetone induces more spherulites at higher temperatures than at lower temperatures. Third, in the high-temperature range ($T_s < T \leq 25$ °C), the data for all doses may be represented by a single line. It is implied that the effect of γ-rays on the structure of polycarbonate is not pronounced at a higher temperature. In this range the heat of mixing is −1.1 kcal/mol.

3.4. Microstructure. Parts a−c of Figure 6 illustrate the microscopic images in polarized light of irradiated polycarbonate swollen by acetone at various temperatures. The arrow indicates the direction of acetone transport. These pictures reveal three regions, i.e., (a) the unswollen core as indicated by the arrow, (b) the swollen zone without any definite morphologic species corresponding to the central black region near the unswollen core, and (c) the crystallization layer between two black regions consisting of many spherulites. The boundary between the crystallization layer and the right-side black region is a free surface. A diffusion front is located at the boundary between the unswollen core and swollen zone. A crystallization front denotes the line between the swollen zone and the crystallization layer. The formation of a sharp front is a phenomenon commonly observed during the mass transport of low molecular weight substances into a glassy polymer. The formation of a sharp front can be

accounted for by the proximity of two zones, i.e., of an unswollen sample core (or of a very slightly swollen sample core) at which the test temperature is above the glass transition temperature T_g and of a zone of the sufficiently swollen polymer which its T_g lies above the tested temperature. When the displacement of the sharp front is proportional to the square root of time, the sharp front is also termed a diffusion front. The acetone transport in polycarbonate alters the stress distribution and microstructure of polycarbonate. The intensity of optical transmittance reflects the stress profile and microstructure. Thus, it is accompanied by a discrete change in optical transmitance from a high value in the unswollen core to a low value in the swollen zone. The separation of the diffusion front and crystallization front provides direct evidence for the presence of a crystallization incubation period which is analogous to that in the case of thermally-induced crystallization of polycarbonate.[37]

The size and population of spherulites at 25 °C are observed in Figure 6 to be more than those at −10 °C; however, the crystallization incubation period of the former is shorter than that of the latter. At −19 °C, the sample does not contain any crystalline morphology. The above observation indicates an increase in the crystallization incubation period with a decreasing test temperature. Acetone at a higher temperature induces more spherlutes and a shorter crystallization incubation period than acetone at a lower temperature. A crystalline structure exerts a strong influence on the solvent absorptin in polycarbonate. A comparison of Figure 4b with Figure 6 indicates that the directions of case II velocity are negative and positive, corresponding to the absence and presence of crystallization, respectively.

3.5. Diffusion Front. The distance X between the diffusion front and free surface is shown in parts a−c of Figure 7 as a square root of time for irradiated polycarbonate with various doses ϕ at temperatures −23 to ~25 °C. Based on the study of Lapčik et al.,[38] the distance X from diffusion front to free surface of the original polycarbonate can be written as

$$X^2 = 2D_f t \tag{5}$$

where t is the swelling time and D_f is the diffusion coefficient for the diffusion front. Results obtained from this calculation are plotted in Figure 8 and satisfy the Arrhenius equation. This figure indicates that three points are worth mentioning. First, the transition temperatures T_f's of slope change are −3, −6, −8, −12, and −14 °C for ϕ = 0, 250, 500, 750, and 1000 kGy, respectively. That is, T_f decreases with an increasing dose. Second, in the low-temperature range (−23 °C ≤ $T < T_f$) the value of D_f increases with an increasing dose at the same temperature; meanwhile, the activation energies are 15, 15, 15, 14, and 15 kcal/mol for ϕ = 0, 250, 500, 750, and 1000 kGy, respectively. This fact implies that the higher dose favors solvent penetration into polycarbonate than a lower dose. However, there is the same mechanism for the diffusion front because they have the same activation energies for all doses within experimental error. Third, in the high-temperature range ($T_f < T \leq$ 25 °C), it is apparent that, within experimental error, the data for all doses may be represented by a single line. The activation energy of D_f in this range is 4 kcal/mol.

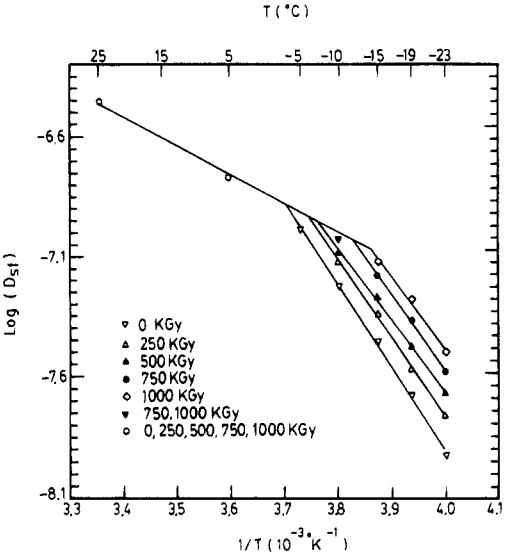

Figure 8. Arrhenius plots of D_f (diffusion front) for different doses.

4. Summary and Conclusions

When acetone transport in irradiated polycarbonate was investigated, the following conclusions were evidenced:

1. The glass transition temperature and molecular weight of irradiated polycarbonate decrease with increasing radiation dose.

2. The activation energy of case I (or case II) has the same value regardless of radiation dose.

3. When acetone induces crystallization in polycarbonate, case II moves from the center to the outer surface. Otherwise, the direction of case II is from the outer surface to the center.

4. Based on the van't Hoff plot, a transition temperature T_s occurs to alter the slope and T_s decreases with an increasing dose. Acetone transport is an exothermic process. Above T_s the equilibrium solubility is independent of radition dose and the heat of mixing is −1.1 kcal/mol. Below T_s the equilibrium solubility decreases with increasing dose; however, the heat of mixing is roughly equal to −6.8 kcal/mol for all doses.

5. According to diffusion front study, a transition temperature T_f occurs to alter the slope and T_f decreases with an increasing dose. T_f is almost equal to T_s for any given dose. Below T_f, the diffusion coefficient for the diffusion front D_f increases with an increasing dose and the activation energy is 15 kcal/mol for all doses. Above T_f, D_f is independent of the radiation dose at any given temperature and the activation energy is 4 kcal/mol.

6. The activation energy for case I (case II and diffusion front) for irradiated polycarbonate is different from that for unirradiated polycarbonate. The heat of mixing for irradiated polycarbonate is also different from that for unirradiated polycarbonate.

Acknowledgment. The authors thank the National Science Council, Taiwan, Republic of China, for financial support through Grant No. NSC 84-2215-E-007-004. J. P. Harmon of University of South Florida for valuable discussions is also acknowledged.

References and Notes

(1) Chapiro, A. *Radiation Chemistry of Polymeric Systems*; Wiley-Interscience: New York, 1962; Chapter VIII.

(2) Ouano, A. C.; Johnson, D. E.; Dawson, B.; Pederson, L. A. *J. Polym. Sci., Polym. Chem. Ed.* **1976**, *14*, 701.
(3) Harrington, R.; Giberson, R. *Mod. Plast.*, **1958**, *36*, 199.
(4) Giberson, R. C. *Mod. Plast.* **1962**, *39*, 143.
(5) Barker, R. E., Jr.; Moulton, W. G. *J. Polym. Sci.* **1969**, *47*, 175.
(6) Crank, J.; Park, G. S. *Diffusion in Polymers*; Acadamic Press: London, 1968.
(7) Roger, C. E. In *Physical and Chemistry of the Organic Solid State*; Fox, D., Labes, M., Weissberger, A., Eds.; Interscience: New York, 1965, Chapter 6.
(8) Hopfenberg, H. B.; Stannett, V. In *The Physics of Glassy Polymers*; Haward, R. N., Ed.; Wiley: New York, 1973; Chapter 9.
(9) Alfrey, T. *Chem. Eng. News* **1965**, *43*, 64.
(10) Frisch, H. L. *Polym. Sci. Eng.* **1980**, *20*, 2.
(11) Thomas, N. L.; Windle, A. H. *Polymer* **1981**, *22*, 627; *Polymer* **1982**, *23*, 529.
(12) Hui, C. Y.; Wu, K. C.; Lasky, R. C.; Kramer, E. J. *J. Appl. Phys.* **1987**, *61*, 5129; *J. Appl. Phys.* **1987**, *61*, 5137.
(13) Hopfenberg, H. B.; Frisch, H. L. *J. Polym. Sci. B* **1969**, *7*, 405.
(14) Ware, R. A.; Tirtowidjojo, S.; Cohen, C. *J. Appl. Polym. Sci.* **1971**, *26*, 2975.
(15) Miller, G. W.; Visser, S. A. D.; Morecroft, A. S. *Polym. Eng. Sci.* **1971**, *11*, 73.
(16) Turska, E.; Benecki, W. *J. Appl. Polym. Sci.* **1979**, *23*, 1619.
(17) Wilkes, G. L.; Parlapiano, J. *Polym. Prepr. (Am. Chem. Soc., Div. Polym. Chem.)* **1976**, *17*, 937.
(18) Turska, E.; Benecki, W. *J. Polym. Sci., Polym. Symp.* **1974**, *44*, 59.
(19) Wang, T. T.; Kwei, T. K. *Macromolecules* **1973**, *6* (6), 919.
(20) Frisch, H. L.; Wang, T. T.; Kwei, T. K. *J. Polym. Sci., Polym. Phys. Ed.* **1969**, *7*, 879.
(21) Wang, T. T.; Kwei, T. K.; Frisch, H. L. *J. Polym. Sci. Polym. Phys. Ed.* **1969**, *7*, 2019.
(22) Kwei, T. K.; Zupko, H. M. *J. Polym. Sci. Polym. Phys. Ed.* **1969**, *7*, 867.
(23) Kwei, T. K.; Wang, T. T.; Zupko, H. M. *Macromolecules* **1972**, *5* (5), 645.
(24) Harmon, J. P.; Lee, S.; Li, J. C. M. *J. Polym. Sci., Part A: Polym. Chem.* **1987**, *25*, 3215.
(25) Harmon, J. P.; Lee, S.; Li, J. C. M. *Polymer* **1988**, *29*, 1221.
(26) Mercier, J. P.; Groeninkx, G.; Lensne, M. *J. Polym. Sci. C* **1963**, *16*, 2059.
(27) Kambour, R. P.; Karasz, F. E.; Daane, J. H. *J. Polym. Sci., Polym. Phys. Ed.* **1967**, *4*, 327.
(28) Turska, E.; Przygocki, W. Faserforsch. Textiltech. **1967**, *18*, 91.
(29) Bluker, P. R.; Sheldon, R. P. *Nature* **1962**, *195*, 172.
(30) Makaruk, L.; Bojarski, J.; Pieniazck, J. *Polymer* **1968**, *56*, 341.
(31) Wu, T.; Lee, S. *J. Polym. Sci., Part B: Polym. Phys. Ed.* **1994**, *32*, 2055.
(32) Kraemer, E. O. *Ind. Eng. Chem.* **1938**, *30*, 1200.
(33) Flory, P. J. *Principles of Polymer Chemistry*; Cornell University Press: Ithaca, NY, 1953; p 310.
(34) Schulz, G. V.; Horbach, A. *Makromol. Chem.* **1959**, *29*, 93.
(35) Flory, P. J. *Principles of Polymer Chemistry*; Cornell University Press: Ithaca, NY, 1953; p 127.
(36) Lin, C. B.; Lee, S. *J. Appl. Polym. Sci.* **1992**, *44*, 2213.
(37) Turska, E.; Hurek, J.; Zmudzinski, L. *Polymer* **1979**, *20*, 321.
(38) Lapčik, L.; Panok, J.; Kellö, V.; Polavka, J. *J. Polym. Sci., Polym. Phys. Ed.* **1976**, *14*, 981.

MA950220A